N-Isopropylacrylamide Decomposition Process in Helium Plasma

H. Martínez, Y. Rodríguez-Lazcano

Instituto de Ciencias Físicas, Universidad Nacional Autónoma de México, Chamilpa 62210, Cuernavaca, Morelos, México

Received 27 April 2006; accepted 31 August 2006
DOI 10.1002/app.25454
Published online in Wiley InterScience (www.interscience.wiley.com).

ABSTRACT: Emission spectroscopy was applied to observe decomposed species of *N*-isopropylacrylamide (NIPAAm) exposed to He plasma, which was generated by AC discharge at the pressure of 400 Pa. As the NIPAAm monomer was exposed to He plasma, light emitted from the NIPAAm and plasma was monitored. In the diagnosis measurement, several emission peaks assigned to the H_α and H_β atomic lines, CH_3O, $CN(B^2\Sigma\text{-}X^2\Pi)$, $CH(A^2\Delta\text{-}X^2\Pi)$, and C_3H_5, CN, CHO, CH_2O, and $C_4H_2^+$ transitions were observed and measured at various discharge times. The present results show the presence of C_4H_2 and $C_4H_2^{+}$*, which are not manifested in great concentration in the simulation of RF acetylene discharge. The time dependence of the emission intensities was also investigated. When the discharge time of He plasma was increased, the emission intensities of the observed transitions also increased and then gradually decreased. © 2006 Wiley Periodicals, Inc. J Appl Polym Sci 103: 2591–2596, 2007

Key words: optical emission spectroscopy; *N*-isopropylacrylamide; pulsed plasma; monomer; glow discharge

INTRODUCTION

It is well known that the interaction of plasma with surface generates a complex mixture of reactive molecules and atoms.[1] Specially, the interaction plasma–polymer produces chemical active species that produce free radicals on the polymer surface,[2,3] resulting in polymer bonds breaking. *In situ* emission spectroscopy provides information of decomposition processes with time exposure to gas plasma. This technique has been applied previously to observe chemical species in plasma–polymer reaction.

The modification of polymer surface exposed to gaseous plasma has been recently studied.[4–6] Kumagai et al.[7] and Kobayashi et al.[8] have reported the decomposition of poly(ethylene terephthalate) and polyacrylonitrile polymers by plasma using emission spectroscopy analysis. Paynter[9] as well as Paynter and Benalia[10] investigated the polystyrene films exposed to oxygen/helium and nitrogen plasmas and they found that the oxygen and nitrogen concentration depth profiles fit to an exponential decay function. Also, oxygen plasma treatment produces functional groups on polystyrene and polydimethylsiloxane films with the formation of low-molecular-weight oxidation products.[11]

Although there is much information about plasma–polymer interaction, little is known about the modification of monomers exposed to plasmas. For this purpose, the NIPAAm monomer has been chosen (Fig. 1), which has been attracting the attention of many authors in relation to its technological and biomedical applications.[12–14] Scientists are working with hydrogels incorporating NIPAAm monomer[15–17] because in water solution and hydrogels it shows low critical solution temperature,[18] around 32°C, close to the human body temperature. This is the reason why NIPAAm-based gels have been used as drug delivery systems.[12]

In the present work we have chosen NIPAAm as the target of plasma treatment. This study describes *in situ* detection of emission species in the NIPAAm-Het plasma reaction process. Hence, the aim of the present work was to determine the emission spectra at the surface of the NIPAAm monomer to characterize the plasma–monomer reaction, since, up to this point, no reports of emission spectroscopy analysis of the plasma were unfortunately made in the presence of NIPAAm monomer.

EXPERIMENTAL

The experimental apparatus and technique to generate the pulse plasma were recently reported.[19] It will be given a brief description here. The system consists of two stainless steel circular plane electrodes, 3 mm thick and 300 mm in diameter. A powder of NIPAAm

Correspondence to: H. Martinez (hm@fis.unam.mx).
Contract grant sponsor: DGAPA; contract grant number: IN-109103.
Contract grant sponsor: CONACyT; contract grant number: 41072-F.

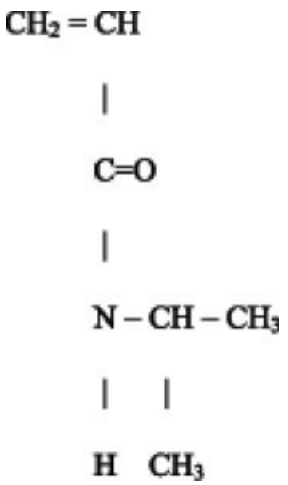

Figure 1 Scheme of the NIPAAm monomer.

(Aldrich Co., USA) monomer sample of about 20 mg was used in this work, which was distributed on the surface of one of the electrode inside of the discharge zone, as a uniform layer of powder of 150 mm diameter and 0.3 mm thickness. The electrodes are positioned at the center of the reaction chamber with a gap spacing of 1 mm. The gas was injected into the reaction chamber through the upper flange. The same gas connection was used for the pressure sensor (MKS, Type 270 signal conditioner and 690A11TRC MKS Baratron) which has a 1333.3 Pa full scale and it can give measurements to about 0.1% of full scale, thus a minimum pressure reading of about 1.33 Pa. AC, 60 Hz discharges generated the plasma in He gas. An ultra-pure He gas (Praxair 99.99%) was used in the course of the measurements. A quartz window was installed on the right lateral flange through which glow discharges were monitored by plasma emission spectroscopy. In front of this quartz window, a 200 mm of focal distance quartz lens (diameter of 25.4 mm) was positioned at 200 mm from the center of the electrodes, and then, the emission light appearing on the NIPAAm and plasma was focused with quartz lens and collected through an optical fiber (solarization-resistant UV fiber with a diameter of 400 μm) connected to the entrance aperture of a high-resolution Ocean Optics spectrometer Model HR2000CG-UV-NIR equipped with a 300 lines mm^{-1} composite blaze grating and a UV2/OFLV-5 detector (2048-element linear silicon CCD array). The grating response has a spectra response in the range of 300–1100 nm with efficiency >30%. The inlet and outlet slits were 5 μm. The wavelength accuracy of the spectrometer was calibrated using an Ar source (Ocean Optics). The data were obtained in a single accumulation of 10 s integration times, which corresponds to 600 times that of the period of pulse voltage. The spectral resolution is 0.035 nm. The spectrum was obtained in step of 0.05 nm. The pulsed plasma was produced in He gas environment at a pressure of 400 Pa. The discharge power supply was maintained at an output of 223 V and a current of 0.12 A (27 W), which was measured using a digital Tektronix multimeter model DM2510. The base pressure of the plasma chamber (6.3×10^{-3} m^3) was 0.60 Pa (measured with a Thermovac sensor TR211 connected to a Termovac TM20 digital controller) using a mechanical pump (Trivac D10, Leybold Pump with nominal pumping speed of 11.8 m^3 h^{-1}) and purged with the working gas several times at 133.3 Pa pressure to remove the background gas.

RESULTS AND DISCUSSION

To observe the decomposition of the NIPAAm monomer exposed to helium plasma, a NIPAAm sample was set on one of the electrodes inside the discharge zone. Before exposing to the plasma, the sample was kept under a vacuum of 0.13 Pa for 10 h. Since NIPAAm has a vapor pressure (88–92°C at 266.6 Pa), therefore it is estimated that the quantity of exposed NIPAAm has a maximum reduction of 15% during the exposure time to vacuum environment. When the monomer sample was exposed to the He plasma, a glow appeared on the monomer surface. Figures 2(a) and 2(b) show the emission spectra of the monomer and the plasma. The detection was carried out at various discharge times of 5, 10, 15, 30, 45, 60, 75, and 100 min at 400 Pa. Figures 2(a) and 2(b) show the emission spectra of the NIPAAm-He system at discharge times of 5, 15, 30, and 100 min. The evolution of the emission lines can be observed as a function of the discharge time. In the 200–1100 nm wavelength region, several emission bands were observed and assigned to[20,21]:

a. CN($B^2\Sigma$-$X^2\Sigma$)(B-X) transitions ($\Delta v = 1,0,-1$) at 360.3, 388.34, 418.10, 421.6, 422.11, 492.51, and 493.94 nm, and to the $A^2\Pi$-$X^2\Sigma$ (A-X) transitions ($\Delta v = 1,0,-1$) at 489.19, 493.56, 504.35, 515.6, 559.78, 584.43, 663.13, 762.41, 790.86, 806.71, 914.06, 918.95, 938.11, and 1096.3 nm.
b. CH($A^2\Delta$-$X^2\Pi$) at 430, 467.9, and 463.44 nm.
c. Formaldehyde (HCHO) at 369.8, 494.7, and 509.7 nm.
d. CH_3O at 413.4 and 364.2 nm.
e. Allyl radical (C_3H_5) to 392.1 nm.
f. $C_4H_2^+$ at 533.04 and 555.11 nm.
g. CHO at 515.27, 520.10, and 557.02 nm.
h. Several emission lines were observed and assigned to H_β and H_α atomic lines at 486.1 and 656.3 nm, respectively.
i. HeI lines at 447.1, 501.6, 587.6, 667.8, 706.5, and 1082.9 nm were observed.

As can be seen from Figure 2, the emission intensities of each transition gradually decreased

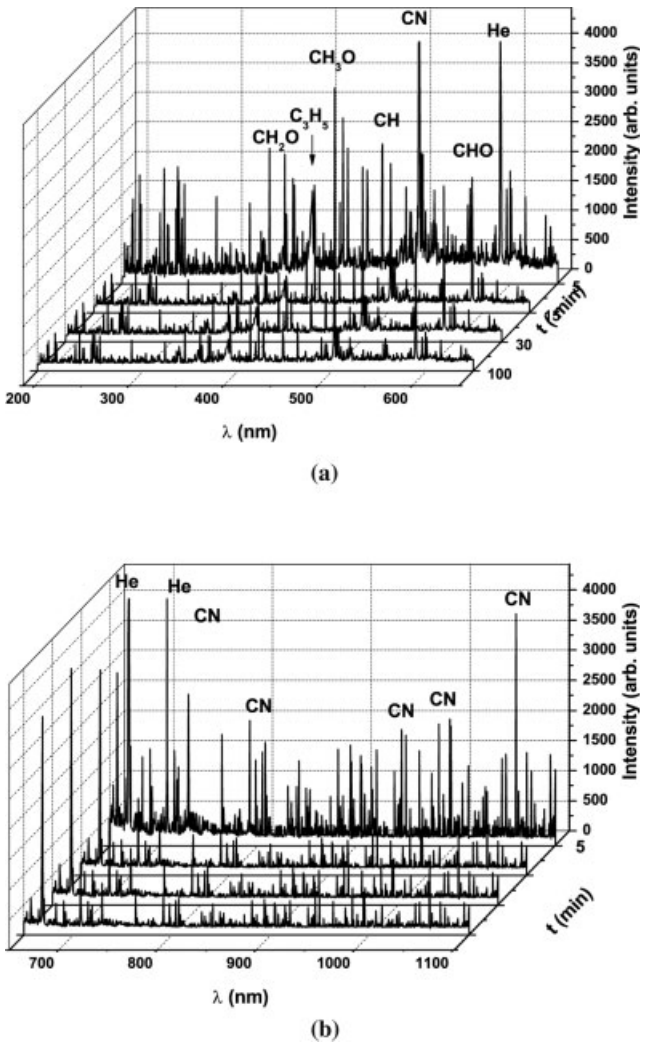

Figure 2 Emission spectra (a) between 200 and 650 nm of NIPAAm He plasma and (b) between 650 and 1100 nm of NIPAAm He plasma.

when the discharge time was increased from 15 to 100 min.

In the monomer and He plasma, the ratio of the intensities of H_α and H_β spectral lines is 4/1, which can be correlated to the ratio of the effective cross sections for the excitation of these lines via the electron impact.[22] The ratio of the intensities of HeI 667.8 and 587.6 nm spectral lines was found to be 1.2. The upper levels of the HeI (^3D, ^1D) lines have an energy of 23.07 eV, whereas the energies of the lower levels of the yellow ($2p\ ^3P_0$) and red ($2p\ ^1P^0_0$) HeI lines are 20.96 and 21.22 eV, respectively. The same intensity of He lines confirms that the species observed (CN, CH, HCHO, CH_3O, C_3H_5, $C_4H_2^+$, and CHO) are produced by NIPAAm monomer decomposition due to the He plasma.

During the experiment, the monomer sample was apparently etched, situation that it can be correlated to the weight decrease of the monomer sample as a function of the discharge time.

Considering the plasma conditions, it can be inferred that excited CN, CH, HCHO, CH_3O, C_3H_5, $C_4H_2^+$, and CHO species play a dominant role in the NIPAAm decomposition process when it was exposed to a He plasma.

In order to understand how the observed species were formed, we point out to the fact that it is well known that the main energy carriers in the glow discharge are due to the free electrons generated by partial ionization of gas partner. They are characterized by a distribution of energies with the average energy of a few electron volts. The population of electron having higher than average energies decreases rapidly with increasing energy. But there will be a small number of electrons that may possess energies of as much as 10–20 eV. The chemical kinetics in NIPAAm-He plasma can lead to many reactions. A variety of species are generated by collisions between the free electrons and the monomer, which include excited molecules, free radicals, and ions. The concentration of free radicals has been found to be five to six orders of magnitude larger than that of the ions; therefore they have been considered[4,23] to be the primary precursors to stable products. This statement was confirmed in the present experiment because the $C_4H_2^+$ species has the lowest intensity. The kinetics involves several different chemical species: electrons (e), positive ions ($C_2H_2^+$, C_2H^+, C_2^+, CH^+, C^+, H^+, H_2^+, He^+, $C_4H_2^+$, $C_6H_2^+$, etc.), radicals (C_4H_2, C_6H_2, CH, CH_2, C_2H, C_2H_3, C_4H_3, C_6H_3, C_4H, C_6H, etc.), atoms (He, O, N, H, C), and molecules (O_2, H_2, C_2, etc.). Because of the great number of active species interacting in He-NIPAAm glow discharge, the experimental rate constants for electron impact dissociation at low energies are not available in general. They can be calculated, in principle, if the dependence of the cross sections with electron energy is well known. Unfortunately, those cross sections are not available for most electron impact neutral dissociation reactions, especially in the low-energy range. On the other hand, the electron energy distribution in glow discharges, usually assumed to be Maxwellian, is not precisely known. This lack of information prevents the knowledge of the exact kinetic scheme of the discharge, and so we may try only to give an explanation of how the observed species were formed. These explanations will be given in the following paragraphs.

The mechanism of He plasma initiated etching is produced by interaction of the electrons, He^+, HeI, and energetic photons (generated in the He plasma) with the monomer surface, that is,

$$(e, He^+, HeI, h\nu) + C_6H_{11}NO \rightarrow 2CH_3 + C_3H_3 + CH + O + N + H + (e, He^+, HeI, h\nu) \quad (1)$$

a) The main process leading to the population of excited CH_3O (that decays to the ground state emit-

ting at 413.4 and 364.2 nm) is through the reaction channel (1), followed by

$$CH_3 + O \rightarrow CH_3O^* \quad (2)$$

Other processes such as $O + O \rightarrow O_2$ and $CH_3 + O + H \rightarrow CH_3OH$ are needed to have the following paths

$$CH_3 + O_2 \rightarrow CH_3O_2 \rightarrow O + CH_3O \quad (3)$$

$$H + CH_3OH \rightarrow CH_3O + H_2 \quad (4)$$

Kerkeni and Clary[24] have studied the dynamics and kinetics of reaction (4) using a quantum mechanical procedure. Marcy et al.[25] have been investigating theoretically and experimentally reaction (2) and Zhu et al.[26] have investigated reaction (3) by *ab initio* orbital theory and variational transition state theory calculation.

b) The observed line at 392.1 corresponding to the C_3H_5 species can be populated via reaction (1), followed by

$$C_3H_3 + CH_3 \rightarrow C_3H_6 \rightarrow H + C_3H_5 \quad (5)$$

The mechanism of radical–radical reaction (5) was studied by quantum chemical methods[27] and Thorn et al.[28] qualitatively observed formation of C_3H_5 as a primary product of reaction (5) at 133.3 Pa. This reaction plays an important role in the mechanisms of evolution of planetary atmospheres.

c) The formation of the $C_4H_2^+$ species can be through the reaction channel (1) followed by neutral gas phase reactions $CH + CH \rightarrow C_2H_2$, electron impact ionization $e + C_2H_2 \rightarrow C_2H_2^+$ and

$$C_2H_2 + C_2H_2^+ \rightarrow H_2 + C_4H_2^+ \quad (6)$$

Herrebout et al.,[29] using a one-dimensional fluid model for an RF acetylene discharge, found that one of the most important ionic species was $C_4H_2^+$ through the reaction channel (6). The ion-neutral reaction (6) is described in detail in Ref. [30]. The present work0 shows the presence of C_4H_2 and $C_4H_2^+$, which are not present in great concentration in the simulation done in Ref. 29 in an RF discharge in acetylene.

d) The presence of HCHO plays an important role in C_2H_4/O_2 flames and in hydrocarbon combustion in general. The decay of HCHO to the ground state emitting at 369.8, 494.7, and 509.7 nm, is through the reaction (1) followed by $CH_3 + CH \rightarrow C_2H_4$, and then by the $O(^3P) + C_2H_4$ reaction. This molecule has been theoretically investigated[31] using various quantum chemical methods, and it was found that one of its major products is through the reaction channel

$$O(^3P) + C_2H_4 \rightarrow HCHO + CH_2 \quad (7)$$

Peeters and Maes,[32] using discharge-flow techniques in combination with molecular beam mass spectrometry, measured the thermal rate coefficients of the reaction (7), and found that at room temperature the rate constant is of $(6.7 \pm 1) \times 10^{-13}$ cm^3 molecule^{-1} s^{-1}.

The CH_2O species can also be produced by

$$CH_3 + O \rightarrow H + HCHO \quad (8)$$

or

$$CH_3 + O \rightarrow CH_3O^* \rightarrow H + HCHO \quad (9)$$

Marcy et al.[25] have investigated theoretically and experimentally both reactions.

Another possible channel studied theoretically by Zhu et al.,[26] using *ab initio* orbital theory and variational transition state theory calculation, is

$$CH_3 + O_2 \rightarrow CH_3O_2 \rightarrow OH + HCHO \quad (10)$$

e) The formation of the HCO species can be through the reaction channel (1) followed by neutral gas phase reactions $CH_3 + CH \rightarrow C_2H_4$ and

$$O(^3P) + C_2H_4 \rightarrow CH_3 + HCO \quad (11)$$

Reaction (11) is also a major product found in the theoretical study[31] based on various quantum chemical methods. Peeters and Maes[32] have measured this reaction.

The HCO species can also be produced by

$$CH_3 + O \rightarrow H_2 + HCO \quad (12)$$

$$CH_3 + O \rightarrow CH_3O^* \rightarrow H_2 + HCO^* \quad (13)$$

which Marcy et al.[25] have been investigating theoretically and experimentally.

Yet, one more possible channel is

$$CH_3 + O_2 \rightarrow CH_3O_2 \rightarrow H_2O + HCO \quad (14)$$

which Zhu et al.[26] have been studied theoretically.

The intensity of the emission bands and lines observed in the emission spectroscopy analysis can be explained correlating all the reactions with their probabilities. Also, some of them may react with other atomic and molecular components to diminish their intensity; for instance, unsaturated hydrocarbons are also known to react with atomic hydrogen, generally by addition in the first step.[23] Hydrogen has also been found to react with compounds of carbon, hydrogen, and oxygen in a variety of ways.[23] One can notice that their mole fractions are somewhat related through type reactions $C_nH_2 + C_2H_2 \leftrightarrows C_{n+2}H_2 + H_2$, so that a decrease by roughly one order of magnitude is observed with addition of a two carbon atoms unit.[33]

Such a variation was evidenced in the difference of intensities of the species observed in the experiment and in rich acetylene–oxygen premixed flames.[34] On the other hand, one of the most important reactions in organic synthesis and polymerization is the well-known addition of an alkyl or other radical to unsaturated hydrocarbons, and the propyl radical then reacts with another ethylene to form the *n*-pentyl radical, and so forth. Another possibility is that reacts in a chain ending with another radical as is typified in common free-radical polymerization processes. Also, a careful examination of bond energies together with the reactions 7, 9, and 11 may be useful to visualize the difference in intensities of the species observed in this experiment. Despite the fact that the C—H bond energy (4.3 eV[4]) is almost two times stronger than the C—N bond energy (2.9 eV[4]) and that C—H is easier to produce in the decomposition of the NIPAAm [see reactions (5) and (6)], there are reactions [(7), (9), and (11)] that diminish the intensity of the CH species and produce the other observed species (C_3H_5, CHO, and $C_4H_2^+$). This condition can give rise to the fact that the intensity of C—N is higher than that of the C—H species. This fact is observed in the present experiment.

Other species such as O, O_2, and CO in their ground and excited electronic states are certainly present and play an important role in the formation of several species observed in the present experiment [see reactions (2), (3), (8), (9), (12),(13), and (14)]. The intensity observed in this work corresponding to O, O_2, and CO species, indicating that they were produced within the pulse plasma, can come from their ground state, or due to the energetic nature of those states, they would result in their lose in collisions or because of reactions with other species to form several species before they can decay under radiation.

It can be seen from Figure 3 that the intensity of the emission lines change as a function of the discharge time (t). The intensities are in the following order CN > CH_3O > CH for $t > 15$ min, and with less intensity respect to the last species, but with almost the same intensity between them are the species H, C_3H_5, CHO, CH_2O, and $C_4H_2^+$. On the other hand, for a $t <$ 15 min, H has the second higher intensity (Fig. 3).

It was confirmed that without monomer the glow discharge of He plasma shows only the strong lines of atomic He in the range of 200–1100 nm.

The emission intensities of some transitions (H 657.35 nm, CN 502.69 nm, CH_3O 413.43 nm, CH 463.44 nm, C_3H_5 392.1 nm, CH_2O 370.98 nm, and CHO 557.02 nm) are shown in Figure 3, as a function of the discharge time. As mentioned before, during the experiment it was observed that the monomer sample was apparently etched. It may be that the weight loss as a function of the discharge time can be related to the intensity variations of the species observed in the experiment, because of their origin from the decomposition of the monomer.

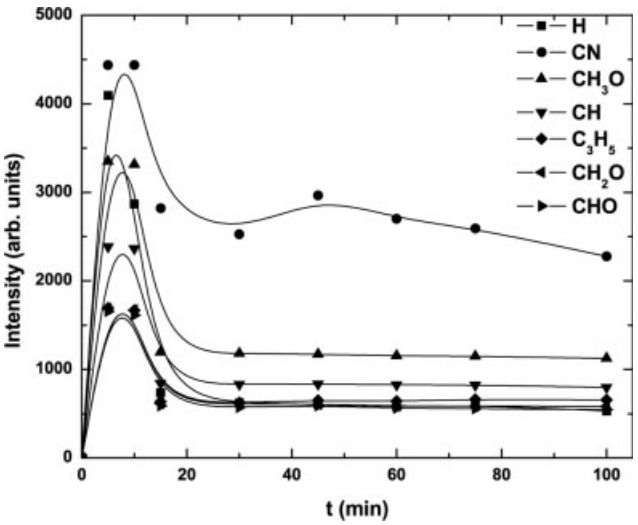

Figure 3 Time profile of emission intensities; solid lines are a smooth fit to the data.

As can be seen from Figure 3, all emission intensities gradually decreased from their peak values, which are reached between 5 and 10 min. At discharges times between 30 and 100 min the intensities of all emission bands became constant; this means that the behavior of the emission intensities may be attributed to the changes in the gas pressure. At the beginning of the plasma exposure, material are removed from the monomer surface by chemical reactions and physical etching at the surface to form volatile products. In the following period, a steady-state etching is established, characterized by a lower desorption of etching products but constant etching rate. It can be observed that the decreasing behavior of all emission lines have the same tendency. By fitting an exponential decay function by least squares to the decreasing behavior of the curves of Figure 3, it was found that all of them have the same tendency: $I(t)\alpha \exp(-t/1.76)$, with a correlation factor of 0.98, indicating that all the transitions decay in the same form. It is clear that they were consumed in the same manner with similar channels reactions as the discharge time increases. The same behavior has been observed recently by Kumagai et al.[7] and Kobayashi et al.[8] in poly (ethylene terephthalate) decomposition process in oxygen, nitrogen, and air plasmas. Similar result was observed in nitrogen and oxygen concentration depth profiles in a time- and angle resolved X-ray photoelectron spectroscopy study of polystyrene exposed to oxygen[9] and nitrogen plasmas.[10]

CONCLUSIONS

The results of the present work focused on the emission spectroscopy analysis of the decomposition of the

NIPAAm monomer exposed to He plasma can be summarized as follows:

a. The emission spectroscopy measurements indicated that the decompositions of the NIPAAm monomer form the following species: H_α, H_β, CH_3O, $CN(B^2\Sigma\text{-}X^2\Pi)$, $CH(A^2\Delta\text{-}X^2\Pi)$, C_3H_5, CN, CHO, CH_2O, and $C_4H_2^+$.
b. For $t > 15$ min, the intensities of the most important emission bands follow the following order $CN > CH_3O > CH$. The intensities of the emission from H, C_3H_5, CHO, CH_2O, and $C_4H_2^+$ are lower, and are almost identical. For $t > 15$ min, the intensity of H is only slightly lower than that of CN.
c. The present work shows the presence of C_4H_2 and $C_4H_2^+$*, which are not present in great concentration in the simulation of an RF acetylene discharge.
d. The results indicate that all the transitions decay in the same form and follow an exponential decay as a function of the discharge time. This suggests that the monomer sample was consumed producing the same products coming from the same reaction channels as the discharge time increase.

The authors are grateful to A. Bustos, A. González, and J. Rangel for technical assistance, and B. E. Fuentes and F. Castillo for helpful suggestions and comments.

References

1. Auciello, O.; Gras-Marti, A.; Valles-Abrarca, J. A.; Flamm D. L. Plasma-Surface Interactions and Processing of Materials; Kluwer Academic: Dordrecht, 1990.
2. Normand, F.; Granir, A.; Leprice, P.; Merec, J.; Shi, M. K.; Clonet, F. Plasma Chem Process 1995, 15, 73.
3. Cho, D. L.; Yasuda H. J Appl Polym Sci 1998, 42, 139.
4. d'Agostino, R. Plasma Deposition, Treatment and Etching of Polymers; Academic Press: New York, 1990.
5. Yasuda, H. K. J Polym Sci Part C: Polym Symp 1988, 42, 46.
6. Chan, C. M.; Ko, T. M.; Hiraoka, H. Surf Sci Rep 1996, 24, 1.
7. Kumagai, H.; Hiroki, D.; Fujii, N.; Kobayashi, T. J Vac Sci Technol A 2003, 22, 1.
8. Kobayashi, T.; Sasama, T.; Wada, H.; Fujii N. J Vac Sci Technol A 2001, 19, 2155.
9. Paynter, R. W. J Elect Spect Rel Phenom 2004, 135, 183.
10. Paynter, R. W.; Benalia, I. H. J Elect Spect Rel Phenom 2004, 136, 290.
11. Marukami, T.; Kuroda, S.; Osawa, Z. J Colloid Interface Sci 1998, 202, 37.
12. Bae, Y. H.; Okamo, T.; Sakurai, Y. Macromol Chem Rapid Commun 1987, 8, 481.
13. Park, T. G.; Hoffman, A. S. J Biomed Res 1990, 24, 21.
14. Gewehr, M.; Nakamura, K.; Ise, N.; Gitano, H. Macromol Chem 1992, 193, 249.
15. Kim, K. H.; Fim, J.; Jo, W. H. Polymer 2005, 46, 2836.
16. Diaz-Peña, E.; Quijada-Garrido, I.; Frutos, P.; Barrales-Rienda, J. M. Macromolecules 2002, 35 2007.
17. Diaz-Peña, E.; Quijada-Garrido, I.; Frutos, P.; Barrales-Rienda, J. M. Polymer 2002, 43, 4341.
18. Schild, H. G. Prog Polym Sci 1992, 17, 163.
19. Martinez, H.; Rosales, I. Surface Eng 2005, 21, 139.
20. Pearse, R. W. B.; Gaydon, A. G. The Identification of Molecular Spectra; Chapman and Hall: London, 1963.
21. Striganov, A. R.; Odintsova, G. A. Tables of Atomic and Ionic Spectral Lines; Energoatomizdat: Moscow, 1982.
22. Stone, P. M.; Kim, Y. K.; Desclaux, J. P. J Res Natl Inst Stand Technol 2002, 107, 327.
23. Boenig, H. V. Plasma Science and Technology; Cornell University Press: Ithaca, NY, 1982.
24. Kerkeni, B.; Clary, D. C. J Chem Phys 2004, 121, 6809.
25. Marcy, T. P.; Diaz, R. R.; Heard, D.; Leone, S. R. J Phys Chem A 2001, 105, 8361.
26. Zhu, R.; Hsu, C. C.; Lin, M. C. J Chem Phys 2001, 115, 195.
27. Stoliarov, S. I.; Knyazev, V. D.; Slagle, I. R. J Phys Chem A 2002, 106, 6952.
28. Thorn, R. P., Jr.; Payne, W. A., Jr.; Chillier, X. D. F.; Stief, L. J.; Nesbitt, F. L.; Tardy, D. C. Int J Chem Kinetics 2000, 32, 304.
29. Herrebout, D.; Bogaets, A.; Gijbels, R.; Goedheer, W. J.; Vanhulsel, A. IEEE Trans Plasma Sci 2003, 31, 659.
30. Vasile, M. J.; Smolinsky, G. Int J Mass Spectrm Ion Phys 1977, 24, 11.
31. Nguyen, T. L.; Vereecken, L.; Hou, X. J.; Nguyen, M. T.; Peeters, J. J Phys Chem A 2005, 109, 7489.
32. Peeters, J.; Maes, D. In Tenth International Symposium on Gas Kinetics, University College of Swansea, July 1988; p A31.
33. Aubry, O.; Delfau, J. L.; Met, C.; Vandenbulcke, L.; Vovelle, C. Diamond Relat Mater 2004, 13, 116.
34. Delfau, J. L.; Vovelle, C. J Chim Phys 1985, 82, 747.